Journal of Engineering Science and Technology
Vol. 13, No. 2 (2018) 309 - 320

3D FINITE ELEMENT MODEL TO PREDICT MACHINING INDUCED RESIDUAL STRESSES USING ARBITRARY LAGRANGIAN EULERIAN APPROACH

PRAKASH MARIMUTHU K.[1,*], THIRTHA PRASADA H. P.[2], CHETHAN KUMAR C. S.[3]

[1]Department of Mechanical Engineering, Amrita School of Engineering, Bangalore, Amrita Vishwa Vidyapeetham, Amrita University, India
[2]Department of Computer Aided Engineering, Visvesvaraya Institute of Advanced Technologies, Visveswaraya Technological University, India
[3]Department of Industrial Engineering Management, M S Ramaiah Institute of Technology, India
*Corresponding Author: prakashkmuthu@gmail.com

Abstract

Understanding the machining process at the microscopic level has been a challenge over the years. The machining process is very complex due to various factors, which are involved like friction, plastic deformation and material failure. The present works aims to develop a 3D Finite Element Model (FEM) to predict the residual stresses induced during the machining operation. Over the years, a lot of development has taken place particularly with the advent of high-end computers and FEM software packages. This work aims to incorporate the developments that have taken place recently in the field of Finite Element Analysis of machining processes and try to introduce an improved model to understand the machining process. Machining induced residual stresses were determined using X-ray diffraction method and compared with the simulation results. Present work is on AISI 1045 steel. Simulation results are in good agreement with the experimental results. Arbitrary Lagrangian Eulerian approach was used for finite element simulations. Many researchers use the orthogonal model to study most of the machining processes; 3D model enables us to see the oblique cutting process. In the present work a 3D model is used in order to be more realistic.

Keywords: Machining; Finite element analysis; Residual stresses; X-ray diffraction.

1. Introduction

Machining is one of the thermo-mechanical deformation processes that leave behind residual stresses in the components. Induced residual stresses affect the

Nomenclatures

A	Yield Stress, Pa
B	Strain Factor, Pa
C	Strain rate factor
D_{1-5}	*Johnson Cook Damage Value constants*
m	*Temperature exponent*
n	Strain exponent
T	Temperature, degree Centigrade
T_{melt}	*Melting Temperature, degree Centigrade*
T_{room}	Room Temperature, degree Centigrade

Greek Symbols

ε	*Strain*
$\dot{\varepsilon}$	*Strain rate, s^{-1}*
$\dot{\varepsilon}_0$	Strain rate threshold value, s^{-1}
ε^{f}	Equivalent plastic strain rate, s^{-1}
μ	Coefficient of Friction
σ	Normal Stress, N/m^2
σ^*	Pressure Stress ratio
τ	Frictional Stress, N/m^2

Abbreviations

AISI	American Iron and Steel Institute
J-C	Johnson Cook

functional performances of the components. Residual stresses can be compressive or tensile, which in turn affect functional performance like creep resistance, fatigue, corrosion resistance and so on [1]. This study attempts to predict the magnitude and type of the residual stresses rising due to machining. The residual stresses induced in components made of AISI 1045 steel, machined using two-flute end mill cutter was measured using X-ray diffraction. Simulation results compared with experimental results were in good agreement.

Residual stresses are the stresses that remain after removing the forces acting on the component. Mechanically generated residual stresses are often a result of manufacturing processes that produce non-uniform plastic deformation. They may develop naturally during processing or treatment, or introduced deliberately to develop a particular stress profile in a component. Examples of operations that produce undesirable surface tensile stresses or residual stress gradients are rod or wire drawing, welding, machining and grinding. Depending upon the nature and magnitude of the induced stresses the performance of the component may vary. The present work aims at determining the nature and magnitude of the induced residual stresses.

The present work uses the arbitrary Lagrangian-Eulerian technique. When using the arbitrary Lagrangian-Eulerian technique in engineering simulations, the computational mesh inside the domains can move arbitrarily to optimize the shapes of elements, while the mesh on the boundaries and interfaces of the domains can move along with materials to precisely track the boundaries and interfaces of a multi-material system.

ALE-based finite element formulations can reduce to either Lagrangian-based finite element formulations by equating mesh motion to material motion or Eulerian-based finite element formulations by fixing mesh in space. Therefore, one finite element code can be used to perform comprehensive engineering simulations, including heat transfer, fluid flow, fluid-structure interactions and metal manufacturing.

2. Literature Survey

Machining induced residual stresses have drawn interest of many researchers [2]. Ulutan and Ozel [3] did an extensive review on the machining induced surface integrity in engineered materials. They observed that there is a large amount of discrepancies between the researchers particularly with regards the nature, magnitude on machining induced residual stresses and further research is need along these lines

Singh and Agrawal [4] did investigations on the induced residual stresses due to deformation machining, a combination of thin structure machining and single point incremental forming/bending in aluminium alloy. Residual stresses was determined using Nano indentation method. Their results showed primarily compressive surface residual stresses in the thin-machined sections.

Kohler et al. [5] studied the machining induced residual stresses in milled titanium parts. He concludes that little knowledge is available about the influence of the machining processes, which induce the residual stresses in components. He also enumerated this of prime importance in the components used in aerospace structures. He used the layer removal method to measure the residual stresses and not the regular X-ray diffraction method as used by many researchers.

The key challenge about residual stresses is prediction and measurement. Lot of research is taking place among the research fraternity. Valiorgur et al. [6] presented an approach in which he predicted residual stresses induced in turning of 316L. He considered a technique that captures the mechanism that generates residual stresses and determines the magnitude of the residual stresses without considering the chip removal process, since it is a very complex phenomenon and simulating it requires high computation time.

Li et al. [7] made an FEM study on the machining induced residual stresses in hardened SKD11 hardened steel. A 2D thermo-mechanical model was developed. The researchers used the Johnson-Cook material model for the simulations and performed experiments to validate the results. They concluded that there was a slight deviation between the experimental and the FEM results.

Abolfazl Zahedi et al. [8] tried to develop a mesh free model to study the effect of crystallographic anisotropy on a response of face centered cubic (f.c.c.) metals to machining. They presented a robust model, which combines the advantages of smooth particle hydrodynamic (SPH) modelling and continuum finite-element approaches.

Agrawal and Joshi [9] made a physics based approach in determining the residual stresses induced in the machining of AISI 4340 steel. They presented an analytical model and concluded that the residual stresses are highly tensile on the machined surface and it is more compressive beneath the machined surface. They made several conclusions on the effect of machining parameters and tool geometry on the residual stresses.

One aspect of residual stress is measurement and the other is determining the factors that influence the machining induced residual stresses. Mohammadpour et al. [10] conducted numerical investigation on orthogonal machining. He used a FE model, to determine the effects of cutting parameters on the induced residual stresses and compared with the available literature. It provides a framework for doing research in machining induced residual stresses. Dahlman et al. [11] studied the influence of cutting parameters and the effect of the rake angle on the residual stresses induced during hard turning. Optimizing the residual stresses is possible by optimizing the cutting parameters and rake angle.

Styger et al. [12] studied the effect of constitutive modelling on the machining induced residual stresses using a 2D finite element model. The work involved the prediction of residual stresses using different materials models for TI6Al4V alloy. Some of the other researches include the prediction of residual stresses after laser assisted machining. The same was also modelled using SPH technique by Balbaa and Nasr [13] Shiozaki et al. [14] whom studied the effect of residual stresses on the fatigue life of steel with punched holes.

Shoba et al. [15] observed that dislocation density had considerable influence on the induced residual stresses. Residual stresses generated during the process of casting is higher than when compared with the residual stresses induced during machining of composites.

Jawahir et al. [16] presented the advancements that have taken place over the years in surface integrity related matters pertaining to metal removal process. Key conclusions from this work are that correlation between the cutting parameters and the functional performances has to be established. Spence and Makhlouf [17] showed how the machining induced stresses would affect the creep characteristics of materials. Their research focused primarily on aluminium alloys. They observed that the distortion of the components lead to creep failure of the components when used in a high temperature environment.

From the literature that is available, the residual stresses induced due to machining have been of interest to many researchers [10]. Understanding the importance of research on residual stresses, the present work is to create a 3D Finite element model to predict machining induced residual stresses in the milling process using ALE approach unlike the traditionally implemented sacrificial layer technique [18].

3. Finite Element Formulation

Finite Element Method (FEM) has helped the researchers significantly in analysing complicated problems. In the area of metal cutting simulations, Finite element simulations have come a long way. FE analyses are of increasing importance for understanding and controlling the manufacturing process. Finite Element Method simulation has been useful in studying the cutting process and observing the chip formation [19, 20]. There are three main Finite Element formulations which are being used by the researchers namely, Lagrangian method, followed by Eulerian method and ALE, that is Arbitrary Lagrangian Eulerian approach. The present works use the ALE approach. In Lagrangian formulation, the Finite element mesh, attached to the work piece, which covers the whole of the region under study. Whenever unconstrained flow of material is involved, such formulation is highly preferred [21-24]; in fluid mechanics, the Eulerian approach, which involves a control volume, is used [25-27]. Arbitrary Lagrangian-Eulerian (ALE) combines the advantages of both the methods [28, 29]. The present work uses the ALE approach to obtain better results.

3.1. Material model

An appropriate material model is essential to represent work material constitutive behaviour [29], the present work uses the Johnson-Cook (J-C) material model [30], along with that it use the Johnson-Cook damage model for the chip to form [31]. Eq. (1) shows the J-C material model.

$$\sigma = (A + B\varepsilon^n)\left(1 + C\ln\frac{\dot{\varepsilon}}{\dot{\varepsilon_0}}\right)\left(1 - \left(\frac{T - T_{room}}{T_{melt} - T_{room}}\right)^m\right) \tag{1}$$

Strain rate, temperature and strain involve in predicting the material responses [32]. The J-C model is the most widely used material models, which predict the material behaviour in the static and dynamic modes [33-36]. Table 1 gives the J-C material model constants for AISI-1045 [37]. In the present work, the tool is a rigid tool, and the research is more about residual stresses that are induced in the work piece. The authors have used a mechanical model to simulate the milling condition while the tool be rigid.

Table 1. Johnson Cook material model constants for AISI 1045 steel.

	A(MPa)	B(MPa)	C	n	m
AISI 1045	553	600	0.0134	0.234	1

3.2. Damage criteria

Material model and Damage model play a significant role in the finite element analysis of the machining process. In the damage model when a parameter pertaining to an element reaches a critical value then it will fail which enables the chip formation [38]. Material model and damage model go hand in hand for the formation of chips during finite element simulation. Damage initiation is a critical parameter and damage evolution is equally critical for the formation of the chip in metal cutting process. In the present work Johnson-Cook damage model along with Johnson-Cook material model is used, Johnson-Cook damage model reads as in Eq. (2)

$$\varepsilon^f = (D_1 + D_2 exp D_3\sigma^*)\left(1 + D_4\ln\frac{\dot{\varepsilon}}{\dot{\varepsilon_0}}\right)\left[1 - D_5\left(\frac{T - T_{room}}{T_{melt} - T_{room}}\right)^m\right] \tag{2}$$

Table 2 gives the values for these constants [35].

Table 2. Johnson-Cook Damage model constants of AISI 1045 Steel.

	D_1	D_2	D_3	D_4	D_5	T_{melt}	T_{room}
AISI 1045	0.06	3.31	-1.96	0.0018	0.058	20◦C	1460◦C

3.3. Friction

Coulomb friction as given in Eq. (3) is used in the work under consideration.

$$\tau = \mu\sigma \tag{3}$$

In the present model, μ is assumed as 0.2.

4. Finite element Model

Finite element analysis reduces the costly experiments, which are required to understand certain phenomenon. In the present work a 3D model was developed. A deformable work piece is of 1×1×0.5 mm. A two-flute end mill cutter of diameter 0.5 mm was the tool; the tool is rigid for the analysis, as our focus is on the residual stresses, which develops in the work piece during machining. The work piece is AISI 1045 steel. C3D8R elements are used in the meshing process (An 8-node linear brick, reduced integration, hourglass control). The mesh is mapped mesh. This type of element and meshing reduces the computation time. Totally 62500 elements were generated. The meshed model is shown in Fig. 1. For the simulation, the base of the work piece was constrained in all degree of freedom. The movement of the tool was constrained in Y and Z direction and the degree of freedom that is free are rotation about the Y-axis and X-axis movement. The cutting conditions were similar to that of the experimental cutting conditions as shown in Table 3. Figure 2 shows the boundary conditions used in the current simulation.

A 3D dynamic explicit analysis ran for 1.5 second. Coulomb friction exists between the tool and the work piece. Surface-to-Node contact exists between the tool and work piece. The result section discusses the results obtained from the simulation.

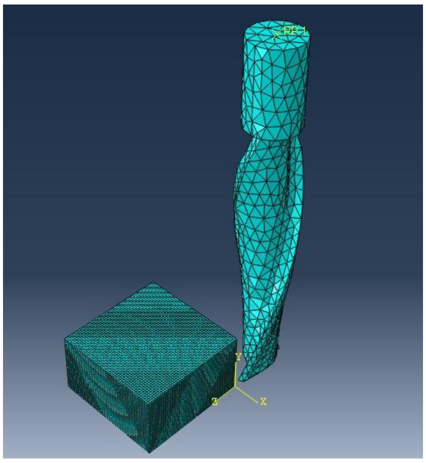

Fig. 1. Meshed model.

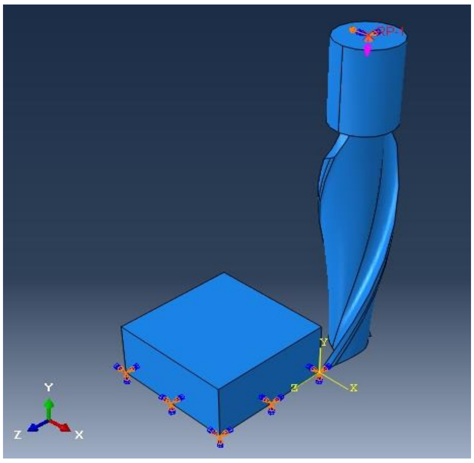

Fig. 2. Model with boundary conditions.

5. Experimental Work

AISI 1045 steel plate machining was accomplished using vertical milling machine. The most critical part of this experimental work was preparing the specimen in such a way that the residual stresses can be measured using the X-ray diffraction method. The specification of the specimen for X-ray diffraction measurement is 24 mm × 24 mm plate of 4 mm thickness. A plate of 50 mm × 60 mm, 6 mm thick AISI 1045 steel plate was taken and then the plate were reduced to the required dimensions. Since plastic deformation induces residual stresses, directly taking the specimen for experimentation will give misleading results, the specimen was first annealed at 750◦C for 2 hours. This procedure is adopted to ensure that the material is free from any stresses induced due to machining the specimen prior to actual experimentation.

After heat treatment, the specimen was milled using a 2 flute tungsten carbide end mill cutter. The cutting parameters are given in Table 3. Figure 3 shows the experimental setup and the finished work piece. The residual stresses induced due to milling were measured using X-ray diffraction [2]. Residual stresses in one un-milled specimen was also measured to ensure that there were no residual stresses in the specimen before machining using the end mill cutter. Results obtained from the experiment are discussed in the results section.

Table 3. Cutting parameters used in the experiment.

Parameter	Value
Speed	1000 rpm
Feed	0.1 mm/rev
Depth of Cut	0.1 mm
Coolant	Dry cutting
Tool Diameter	3 mm
Tool Type	2 flute End mill

Fig. 3. Experimental setup and finished work piece.

6. Results

The process of determining the residual stresses through any experimental method is very cumbersome process, it involves careful preparation of specimens. The procedure generally involves, ensuring or zero residual stresses before going for the actual machining process, which many a time may not be the case. Followed by residual stress measurement by X-ray diffraction method or hole drilling method or hardness determination method etc. Even after doing so, one may be able to determine the stresses at one point on a plane only. However, by using the Finite element method one will be able to come over these obstacles since the model considered for the machining process is free of residual stresses. We can get the residual stresses across the depth of the specimen even at micron distance. The cost of experimental testing for one specimen across the depth is very high and one is not sure of the values because of the high expertise required to interpret the values. Sometimes one may have to repeat the experiment to be sure of the obtained values. The model developed in this work will remove some of the obstacles in determining the nature and magnitude of the residual stresses.

The machining induced residual stresses were measured in un-milled and milled work piece. The un-milled work piece the residual stresses (principle stresses) were found to be 5.6 ±4.5MPa (compressive stresses) and that of the milled specimen using the parameters in Table 3 was found to be 175.5±15.9 MPa (compressive stresses). The measured residual stresses are compared with the simulation results. The experimental results were in good agreement to the simulation results.

The maximum residual stress obtained after machining using the Finite element model was 148 MPa (compressive stresses); just beneath the machined surface, the stresses are tensile and then becomes compressive. The simulated results are in good agreement with the experimental results. There is a small variation in the experimental and the simulation results, which could have arisen because a mechanical model was used for the simulation purposes. The Von Mises stress distribution is shown in Fig. 4. Figure 4 shows how the material has been removed and the stress distribution. The residual stress distribution is shown in Fig. 5.

Figures 4 and 5 are reduced models. The stress distribution computed on the entire model is show in Fig. 6. An average force of 2N was predicted for the milling operation using the Finite Element Model.

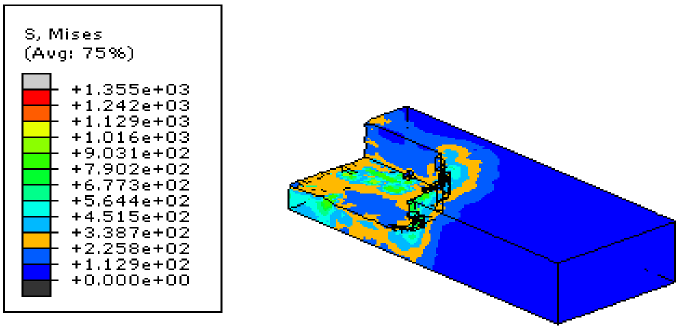

Fig. 4. Von Mises stress distribution on the milled work piece.

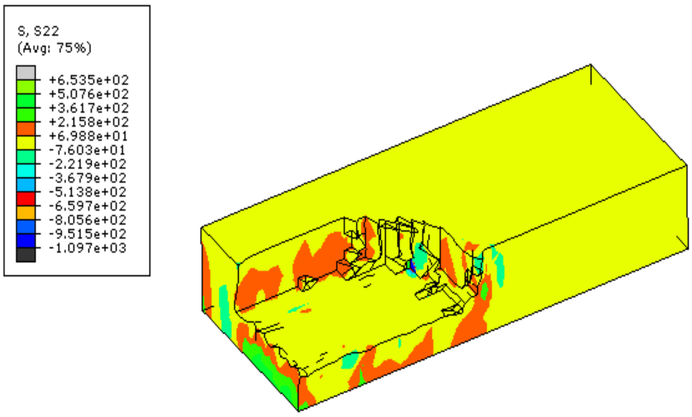

Fig. 5. Residual stresses distribution on in the milled work piece.

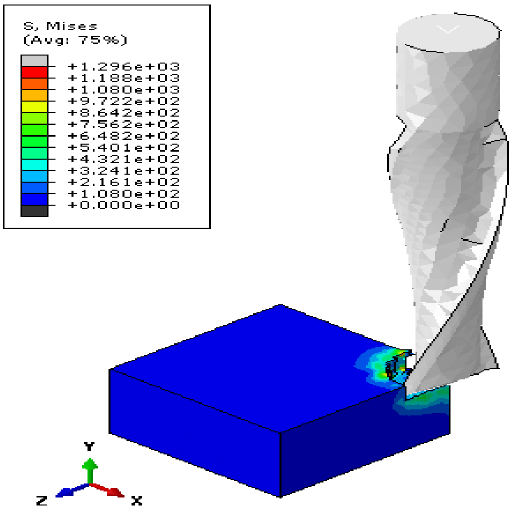

Fig. 6. Von Mises stress distribution- full model.

7. Conclusion and Future work

The present work predicts the residual stresses induced by milling operation on AISI 1045 steel. A 3D model using Abaqus Explicit commercially available software was developed. J-C material model and J-C Damage model was used for the Finite Element analysis. Unlike many of the researches sacrificial layer was not used rather, the ALE approach was used to give a realistic picture of the process. Extra care was taken for the preparation of the specimens to ensure proper measurement of the residual stresses using X-ray diffraction method. The experiment and the simulation results were in good agreement with each other. Future work includes, developing a coupled thermo-mechanical model. A model to determine the effect of the induced residual stresses on the functional performance of the material need to be developed.

References

1. Varela, P.I.; Rakurty, C.S.; and Balaji, A.K. (2014). Surface integrity in hard machining of 300M steel: Effect of cutting-edge geometry on machining induced residual stresses. *Procedia CIRP*, 13, 288-293.
2. Arrazola, P.J.; Kortabarria, A.; Madariaga, A.; Esnaola, J.A.; Fernandez, E.; Cappellini, C.; Ulutan, D. and Özel, T. (2014). On the machining induced residual stresses in IN718 nickel-based alloy: Experiments and predictions with finite element simulation. *Simulation Modelling Practice and Theory*, 41, 87-103.
3. Ulutan, D.; and Ozel, T. (2011). Machining induced surface integrity in titanium and nickel alloys: A review. *International Journal of Machine Tools and Manufacture*, 51(3), 250-280.
4. Singh, A.; and Agrawal, A. (2015). Investigation of surface residual stress distribution in deformation machining process for aluminum alloy. *Journal of Materials Processing Technology*, 225, 195-202.

5. Köhler, J.; Grove, T.; Maiß, O.; and Denkena, B. (2012). Residual stresses in milled titanium parts. *Procedia CIRP*, 2, 79-82.
6. Valiorgue, F.; Rech, J.; Hamdi, H.; Gilles, P.; and Bergheau, J.M. (2007). A new approach for the modelling of residual stresses induced by turning of 316L. *Journal of Materials Processing Technology*, 191(1-3), 270-273.
7. Li, J.L.; Jing, L.L.; and Chen, M. (2009). An FEM study on residual stresses induced by high-speed end-milling of hardened steel SKD11. *Journal of Materials Processing Technology*, 209(9), 4515-4520.
8. Abolfazl Zahedi, S.; Demiral, M.; Roy, A.; and Silberschmidt, V.V. (2013). FE/SPH modelling of orthogonal micro-machining of f.c.c. single crystal. *Computational Materials Science*, 78, 104-109.
9. Agrawal, S.; and Joshi, S.S. (2013). Analytical modelling of residual stresses in orthogonal machining of AISI4340 steel. *Journal of Manufacturing Processes*, 15(1), 167-179.
10. Mohammadpour, M.; Razfar, M.R.; and Jalili Saffar, R. (2010). Numerical investigating the effect of machining parameters on residual stresses in orthogonal cutting. *Simulation Modelling Practice and Theory*, 18(3), 378-389.
11. Dahlman, P.; Gunnberg, F.; and Jacobson, M. (2004). The influence of rake angle, cutting feed and cutting depth on residual stresses in hard turning. *Journal of Materials Processing Technology*, 147(2), 181-184.
12. Styger, G.; Laubscher, R.F.; and Oosthuizen, G.A. (2014). Effect of constitutive modeling during finite element analysis of machining-induced residual stresses in Ti6Al4V. *Procedia CIRP*, 13, 294-301.
13. Balbaa, M.A.; and Nasr, M.N.A. (2015). Prediction of residual stresses after laser-assisted machining of inconel 718 using SPH. *Procedia CIRP*, 31, 19-23.
14. Shiozaki, T.; Tamai, Y.; and Urabe, T. (2015). Effect of residual stresses on fatigue strength of high strength steel sheets with punched holes. *International Journal of Fatigue*, 80, 324-331.
15. Shoba, C.; Ramanaiah, N.; and Rao, D.N. (2015). Influence of dislocation density on the residual stresses induced while machining Al/SiC/RHA hybrid composites. *Journal of Materials Research and Technology*, 4(3), 273-277.
16. Jawahir, I.S.; Brinksmeier, E.; M'Saoubi, R.; Aspinwall, D.K.; Outeiro, J.C.; Meyer, D.; Umbrello, D.; and Jayal, A.D. (2011). Surface integrity in material removal processes: Recent advances. *CIRP Annals - Manufacturing Technology*, 60(2), 603-626.
17. Spence, T.W.; and Makhlouf, M.M. (2015). The effect of machining-induced residual stresses on the creep characteristics of aluminum alloys. *Materials Science and Engineering: A*, 630, 125-130.
18. Jalili Saffar, R.; Razfar, M.R.; Zarei, O.; and Ghassemieh, E. (2008). Simulation of three-dimension cutting force and tool deflection in the end milling operation based on finite element method. *Simulation Modelling Practice and Theory*, 16(10), 1677-1688.
19. Fang, G.; and Zeng, P. (2005). Three-dimensional thermo–elastic–plastic coupled FEM simulations for metal oblique cutting processes. *Journal of Materials Processing Technology*, 168(1), 42-48.

20. Maranhão, C.; Paulo Davim, J. (2010). Finite element modelling of machining of AISI 316 steel: Numerical simulation and experimental validation. *Simulation Modelling Practice and Theory*, 18(2),139-156.
21. Krishnakumar, P.; Marimuthu, K.P.; Rameshkumar, K.; and Ramachandran, K.I. (2013). Finite element simulation of effect of residual stresses during orthogonal machining using ALE approach. *International Journal of Machining and Machinability of Materials*, 14(3), 213-229.
22. Ezilarasan, C.; Senthil kumar, V.S.; and Velayudham, A. (2014). Theoretical predictions and experimental validations on machining the Nimonic C-263 super alloy. *Simulation Modelling Practice and Theory*, 40, 192-207.
23. Maurel-Pantel, A.; Fontaine, M.; Thibaud, S.; and Gelin, J.C. (2012). 3D FEM simulations of shoulder milling operations on a 304L stainless steel. *Simulation Modelling Practice and Theory*, 22, 13-27.
24. Bharathwaj, R.; Giridharan, P.; Karthick, K.; Prasath, C.H.; and Marimuthu, K.P. (2016). Computational study of Coanda based Fluidic Thrust Vectoring system for optimising Coanda geometry. *IOP Conference Series: Materials Science and Engineering*, 149, 012210.
25. Movahhedy, M.R.; Gadala, M.S.; and Altintas, Y. (2000). Simulation of chip formation in orthogonal metal cutting process: An ALE finite element approach. *Machining Science and Technology*, 4(1), 15-42.
26. Meyappan, P.L.; Roy, A.; Abhijith, J.; Ramesh, M.N.V.; and Prakash Marimuthu, K. (2015). Tsunami wave impact on structures. *International Journal of Applied Engineering Research*, Special Issue,10(50), 1135-1139.
27. Ramon Codina; Guillaume Houzeaux; Herbert Coppola-Owen; Joan Baiges. (2009). *Journal of Computational Physics*, 228, 1591-1611.
28. Özel, T.; and Zeren, E. (2004). Determination of work material flow stress and friction for FEA of machining using orthogonal cutting tests. *Journal of Materials Processing Technology*, 153-154, 1019-1025.
29. Opoz, T.T.; and Chen, X. (2010). Finite element simulation of chip formation. *School of Computing and Engineering Researchers' Conference*, University of Huddersfield, UK.
30. Xi, Y.; Bermingham, M.; Wang, G.; and Dargusch, M. (2013). Finite element modeling of cutting force and chip formation during thermally assisted machining of Ti6Al4V Alloy. *Journal of Manufacturing Science and Engineering*, 135(6), 061014.
31. Yue, C.X.; Liu, X.L.; Jia, D.K.; Ji, S.Y.; and Zhai, Y.S. (2009). 3D finite element simulation of hard turning. *Advanced Materials Research*, 69-70, 11-15.
32. Ben Mcclain, S.A.B.; and Maldonado, G.I. (2002). A numeric investigation of the rake face stress distribution in orthogonal machining. *Journal of Materials Processing Technology*, 123, 114-119.
33. Milani, A.S.; Dabboussi, W.; Nemes, J.A.; and Abeyaratne, R.C. (2009). An improved multi-objective identification of Johnson–Cook material parameters. *International Journal of Impact Engineering*, 36(2), 294-302.
34. Daoud, M.; Chatelain, J.F.; Bouzid, A. (2017). Effect of rake angle-based Johnson-Cook material constants on the prediction of residual stresses

and temperatures induced in Al2024-T3 machining. *International Journal of Mechanical Sciences*, 122, 392-404.

35. Ye, G.G.; Xue, S.F.; Ma, W.; Jiang, M.Q.; Ling, Z.; Tong, X.H.; and Dai, L.H. (2012). Cutting AISI 1045 steel at very high speeds. *International Journal of Machine Tools and Manufacture*, 56, 1-9.
36. Prakash Marimuthu, K.; Chethan Kumar, C.H.; and Thirtha Prasada H.P. (in press). 2D finite element thermo-mechanical model to predict machining induced residual stresses using ALE approach. *Materials Today: Proceedings*.
37. Prakash Marimuthu, K.; Thirtha Prasada H.P.; and Chethan Kumar, C.H. (2017). Force, stress prediction in drilling of AISI 1045 steel using Finite Element Modelling. *IOP Conf. Ser.: Mater. Sci. Eng,* 225, 012030.
38. Duan, C.Z.; Yu, H.Y.; Cai, Y.J.; and Li, Y.Y. (2010). Finite element simulation and experiment of chip formation during high speed cutting of hardened steel. *AMM*, 29-32, 1838-1843.